3.17 AN OBJECTIVE NOWCASTING TOOL THAT OPTIMIZES THE IMPACT OF SATELLITE DERIVE SOUNDER PRODUCTS IN VERY-SHORT-RANGE FORECASTS

Ralph Petersen[*1] and Robert Aune[2]
[1] Cooperative Institute for Meteorological Satellite Studies (CIMSS),
University of Wisconsin – Madison
[2] NOAA/NESDIS/ORA, NESDIS/Advanced Satellite Products Team, Madison, Wisconsin

1. BACKGROUND

Many future instruments (e.g., Wind Profilers networks, automated aircraft reports and the Hyperspectal Environmental Sounder planned for GOES-R) have the capability of resolving atmospheric features beyond today's capabilities in both time and space. Although these data are expected to generate improvements in numerical forecast guidance out to 48 hours and beyond, a greater benefit from these high-time-frequency and detailed data sources may come from their use in real time objective nowcasting systems designed to assist forecasters with identifying rapidly developing, small-scale extreme weather events.

These nowcasting systems will need to detect and retain extreme variations in the atmosphere, incorporate large volumes of high-resolution asynoptic data from satellites and other high-resolution systems, and be very computationally efficient. Accomplishing this will require numerical approaches and techniques that are notably different from those used in numerical weather prediction where the forecast objectives cover longer time periods. The nowcasting systems will need to place an emphasis on retaining the integrity of individual observations and preserving the large gradients seen in these data through time. Speed, however, will be of the essence, since in many cases the detailed information provided in the observations is extremely perishable and rapid and frequent updates are essential in the field.

The basis for a new approach to objective nowcasting is presented that uses lagrangian techniques to optimize the impact and retention of information provided by multiple observing systems. Real-data tests are shown in which GOES Derived Product Imagers (DPIs) of multi-layer precipitable water observations are used with the goal of identifying horizontal and vertical details of the environments associated with the onset of significant weather events several hours in advance. These data serve as surrogates for products from the upcoming GOES-R ABI, while tests with AIRS data can provide insight into the additional benefit that might be gained from a future GOES hyperspectral sounder.

* *Corresponding author address:* Dr. Ralph A. Petersen, University of Wisconsin-Madison, Cooperative Institute for Meteorological Satellite Studies (CIMSS), 1225 West Dayton Street, Madison, WI 53706;
Email Ralph.Petersen@SSEC.WISC.EDU;
Phone (608) 262-5152; Fax (608)-262-5974.

2. BASIS FOR LAGRANGIAN NOWCASTING

The Lagrangian Objective Nowcasting system described here is designed both to retain extreme variations in observed atmospheric parameters and preserve vertical and horizontal gradients observed in the various data fields throughout a 3 to 6 hr projection. Instead of relying on traditional Eulerian approaches which forecast the changes in parameters at fixed grid points and which require that observations be interpolated from their original locations to the fixed grid (and thereby lose some of their detail and data extremes), the approach used here applies the equations of motion ***directly to parcels originating at their points of observations***.

The lagrangian approach is based on the Discrete Model Theory (Greenspan, 1972) and has been shown to be an effective diagnostic tool by Kocin et al., 1986. In thier study, low- and upper-level trajectories were obtained during a pre-convective period based using special 3-hourly rawinsonde data. The result (Fig. 1) not only showed that the lagrangian approach can simulate the interplay between dry line approaching from west and transport of Gulf moisture from the south using relatively long (15 minute) time steps, but also the coincidence of the low-level moisture convergence with drying and the l divergence in the exit region of the jet streak aloft (not shown).

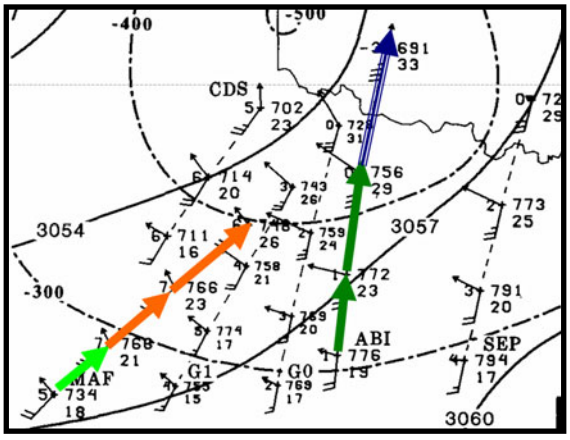

Fig. 1. Example of lower-tropospheric parcel flow preceding 10 April 1979 tornado outbreak over extreme southwestern OK. Note acceleration of moist, ascending air from ABI being simultaneously approached by dry descent air originating at MAF. (From Kocin et al., 1986.)

2.1 Model Formulation

In discrete form (See Petersen and Uccellini, 1979), the basic equations of motion become:

$$a_x^{(t)} = - \Delta\Psi^{(t)} / \Delta x + f^{(t)} v^{(t)},$$
$$a_y^{(t)} = - \Delta\Psi^{(t)} / \Delta y - f^{(t)} u^{(t)}, \quad \text{or}$$

$$v^{(t)} = 1/f^{(t)} [a_x^{(t)} + \Delta\Psi^{(t)} / \Delta x],$$
$$u^{(t)} = -1/f^{(t)} [a_y^{(t)} + \Delta\Psi^{(t)} / \Delta y].$$

In discrete model formulation (Greenspan (1972), the future momentum and location of parcels is calculated using energy conservative formulae:

$$u^{(t+1)} = u^{(t)} + \Delta t [1.5 a_x^{(t)} - 0.5 a_x^{(t-1)}],$$
$$v^{(t+1)} = v^{(t)} + \Delta t [1.5 a_y^{(t)} - 0.5 a_y^{(t-1)}], \quad \text{and}$$

$$x^{(t+1)} = x^{(t)} + 0.5 \Delta t [u^{(t)} + u^{(t+1)}],$$
$$y^{(t+1)} = y^{(t)} + 0.5 \Delta t [y^{(t)} + y^{(t+1)}],$$

where for the first time step

$$u^{(1)} = u^{(0)} + a_x^{(0)} \Delta t, \text{ and } v^{(1)} = v^{(0)} + a_y^{(0)} \Delta t.$$

At each time step, $a_x^{(t)}$ and $a_y^{(t)}$ are calculated by interpolating $\Delta\Psi/\Delta x$ and $\Delta\Psi/\Delta y$ bi-linearly from a regular grid to each parcel location, f is calculated from latitude location of the parcel, and the parcel accelerations are calculated arithmetically at time t and saved for time use in the next step as t-1.

2.2 Analytical Tests

Extensive analytical tests were performed to document the ability of the method to retain gradients and data field maxima/minima through advection. These tests not only quantified the computational efficiency of the lagrangian approach and the ability of the approach to retain observed gradients and isolated maxima and minima, but also demonstrated that the technique eliminates amplitude and phase error biases associated with the advection of very small wavelength features which occur when using conventional Eulerian techniques. The cost/benefit diagram in Figure 2 shows that an optimal time step for the lagrangian technique is about 600-700 seconds, independent of data density.

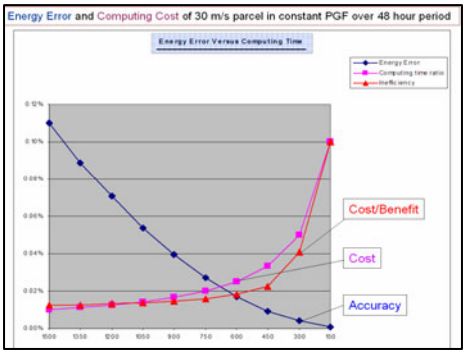

Fig. 2. Comparisons of errors in energy conservation and computational time step for idealized lagrangian test cases.

Additional analytical tests have been conducted to determine the advantage of lagrangian techniques to different dynamical processes especially relevant to nowcasting. Specific emphasis was placed on modeling the structure of the Jet Streak. The goals of these examples are two-fold: 1) to provide evidence of the advantage of the approach in a manner relevant to forecasters and 2) to provide a tools for teaching a more thorough understanding of the dynamical processes involved in mesoscale systems – especially those related to creating an environment conducive to severe storm development – and how these dynamics are shown in rapidly changing GOES water vapor imagery.

For example, analyses of parcels entering an idealized jet streak reveal a variety of features which modulate as the strength of the jet streak increases. Figure 3 shows a number of examples typical of more extreme shear conditions. Impacts include asymmetry in the divergence/convergence couplets around the jet streak, and enhanced upper-level convergence on the anticyclonic side of the jet streak divergence ahead of it.

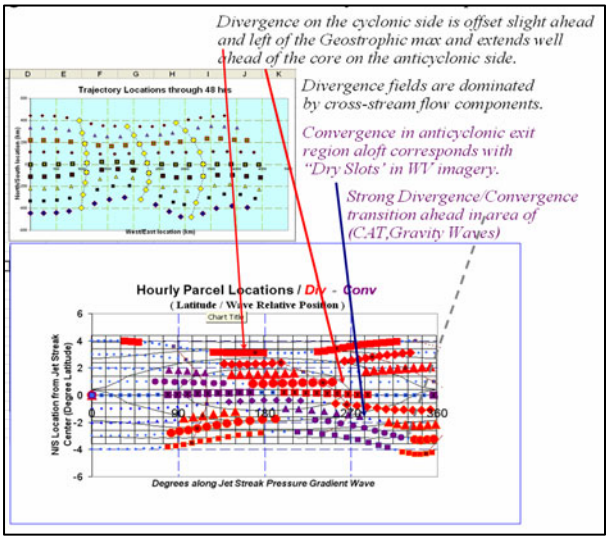

Fig. 3. Example of test of lagrangian system with analytical Jet Streak, including annotations of specific findings.

It is noteworthy that the development of this feature has occurred using parcels which had been initially in complete dynamical balance and which were initially separated by 111 km. In the exit region, the separation decreases to less than 10 km. Producing such a simulation with an Eulerian system would have required grid resolutions of ~1-2 km – an extremely resource intensive effort – while the lagrangian approach was done nearly instantaneously on a PC.

These analytical tests show that the lagrangian approach is extremely computationally efficient (since the inertial advective terms needed in Eulerian models no longer dictate that the model time step must be a function of grid spacing), is able to retain sharp gradients and observed maxima and minima, and has the capability of providing timely updates to guidance provided by operational forecast models.

3. REAL DATA TESTS USING GOES DERIVED PRODUCT IMAGE MOISTURE DATA

Real data tests are currently being conducted at CIMSS - with the goals of identifying details of the environments associated with the onset of significant weather events several hours in advance. The tests use full resolution (10 km) derived layer moisture products from the GOES-10/12 sounders to update and enhance operational RUC forecasts. Initial tests are focusing on the use of multi-layer GOES Derived Image Product (DPI) moisture data, with the long-term goal of providing a basis for using GOES-R and NPOES data when they arrive.

The objective of these tests is to provide forecasters 3 to 6 hour predictions of the DPI fields which can be updated every hour. Initial application of the lagrangian Nowcasts focuses on the optimal approaches for providing *updates of existing mesoscale model outputs in the free-atmosphere by combining the power of Short-Range NWP with detail and frequency of satellite observation updating*. This is done by matching of RUC-II wind analyses and geopotential analyses/forecasts with GOES Sounder (DPI) Water Vapor Data. (It should be noted that the GOES Sounder profiles are not currently used in RUC over land.) Individual air parcels are assigned to each GOES-DPI data location and marched forward in time at 15 minute intervals. Note that additional observations can be included as they arrive to provide additional data points since the satellite data arrive every 30-60 minutes.

The case presented here considers the isolated hail storm event that caused major property damage across southern Wisconsin at about 0300 UTC 14 April 2006. Visible satellite (Figure 5) imagery during the day shows that the surrounding area was nearly devoid of other cloud features, making it optimal for satellite sounding retrieval. Conventional NWP guidance showed little evidence of precipitation in the area. The important questions are both 1) *where* and *when* severe convection *will* occur, and 2) *where* convection *will NOT* occur?

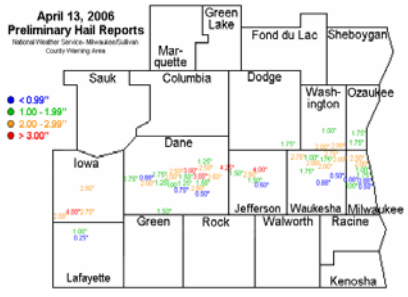

Fig. 4 Hail reports from the evening of 13 April 2006.

The evolution of IR Imagery in Figure 6 shows that by the time of the hailstorm development over southwestern WI, much of the area was almost entirely obscured by cirrus originating from a separate area of convection that developed earlier over IA, producing a weak tornado there, as well as earlier storms in extreme south-western WI. The masking of the middle and lower-troposphere moisture and mid-level dryness by the cirrus clouds made the satellite data being viewed by forecasters immediately before the storm developments far less useful than it might have been had the cirrus clouds not been present. This limitation is alleviated using nowcasts of multi-level GOES DPI Precipitable Water data from before the storm formation.

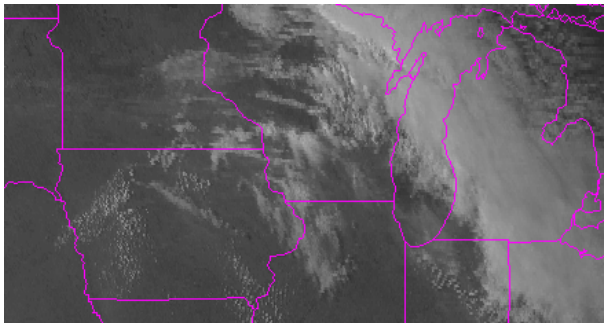

Fig. 5 GOES Visible imagery for 2115 UTC on 13 April 2006.

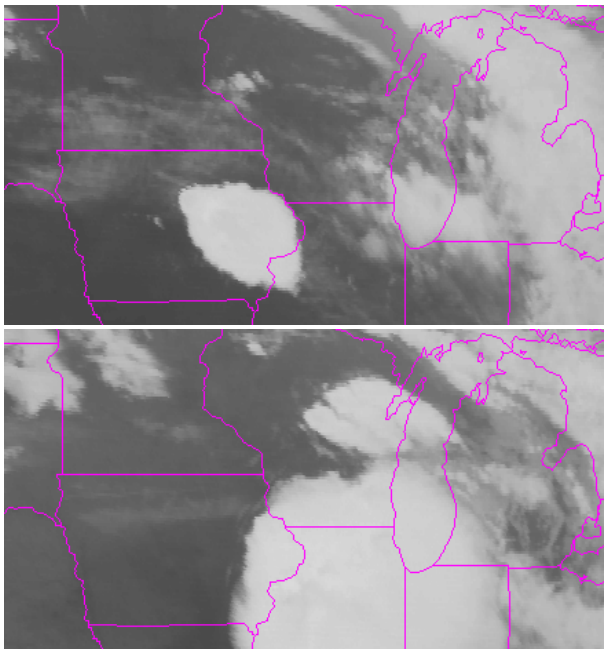

Fig. 6 GOES IR images from 0015 UTC (top) and 0315 UTC (bottom) on 14 April 2006.

In an attempt to assess whether the nowcasting system can project the satellite information available in clear areas earlier in the day into the areas of subsequent storm development (but without the limiting effects of cirrus contamination), the lagrangian nowcasting system was initialize with parcels assigned to every observational point in the 10km resolution GOES DPI PW imagery at 2100 UTC 13 April 2006. RUC-II winds were interpolated to each parcel location and dynamic parcel trajectories were calculated using the initial RUC wind data and observed height field tendencies. Layer averaged data from 850-750 hPa and 550-450 hPa

were used to initialize each GOES DPI observation See figure 7 as an example).

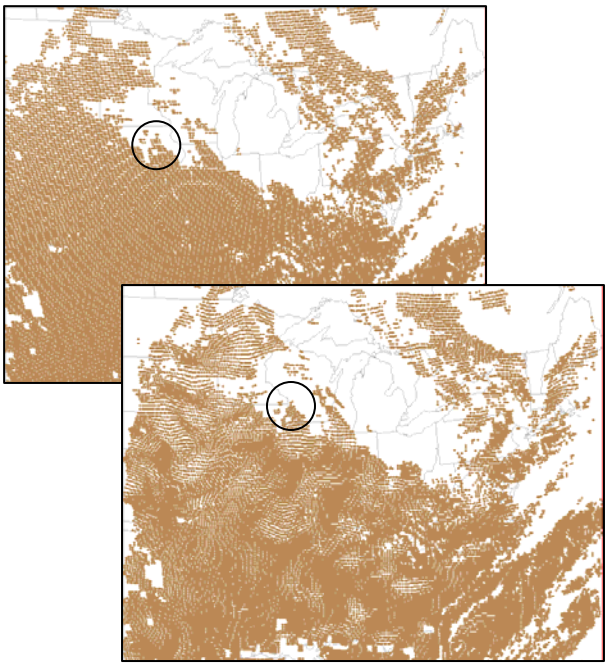

Fig. 7 Illustration of nowcast domain with initial (top) and 2-hr (bottom) locations of low-level (900 – 700 hPa) parcels used in nowcasts initialized at 2100 UTC 13 April 2006.

Three and six hour nowcasts of the middle- and lower-level PW depict the translation of the parcels from afternoon into evening. The nowcast images clearly show the movement of the moisture maximum initially in central IA (blue areas left column of figure 8) east-north-eastward into southwestern WI during the 6 hours between 2100 and 0300 UTC. Simultaneously, the region of upper-level dryness initially over NE (dark red areas in right column of figure 8) has also moved into this area, showing a distinct concentration in the area when convection subsequently developed.

The nowcast images are created by interpolating the precipitable water from each projected parcel location onto a fixed 10 km grid and then color-coding the grid field. (Note the movement of the area of moist parcels circled in figure 7 from central to north-eastern IA in the first 2 hours of the nowcast, and the corresponding change in depiction of the top initial and 2 hr nowcast images in figure 8.) In order to preserve information from previous nowcast, the interpolation process uses grids from the last hourly sequence of nowcasts valid at the same times as 'first guess' fields for the new images.

The development of convective instability is vital to the development of isolated severe convective storms such as this. The convective destabilization process is a complex one, in which differential motions of mid-level warm dry air over regions of moister air nearer the surface can create isolated areas of convective instability,. Not only must there be a local concentration in moisture at low levels, but the moisture must first be capped by increasing subsidence of dry air from aloft during the time while the low level moisture is concentrating in an area. This creates the convectively unstable environment suitable for severe convection. It is advantageous to have the upper-level drying slightly out of phase with the area (initially lagging) of progression of the area of low-level moisture flux convergence.

For the convection to occur, however, the low level moisture must be able to break through the overlying subsidence inversion. This can occur by having sufficient low level convergence present to lift the inversion while convective clouds are forming below. This process must also be monitored using available real-time wind observations.

Study of the nowcast images for this case show that was indeed the case for this example. The increase of low-level moisture was almost coincident with the development of convection, while the concentration of middle-level dryness occurs only slightly before the convection redeveloped there, followed by a movement of the dryness coming from farther to the west.

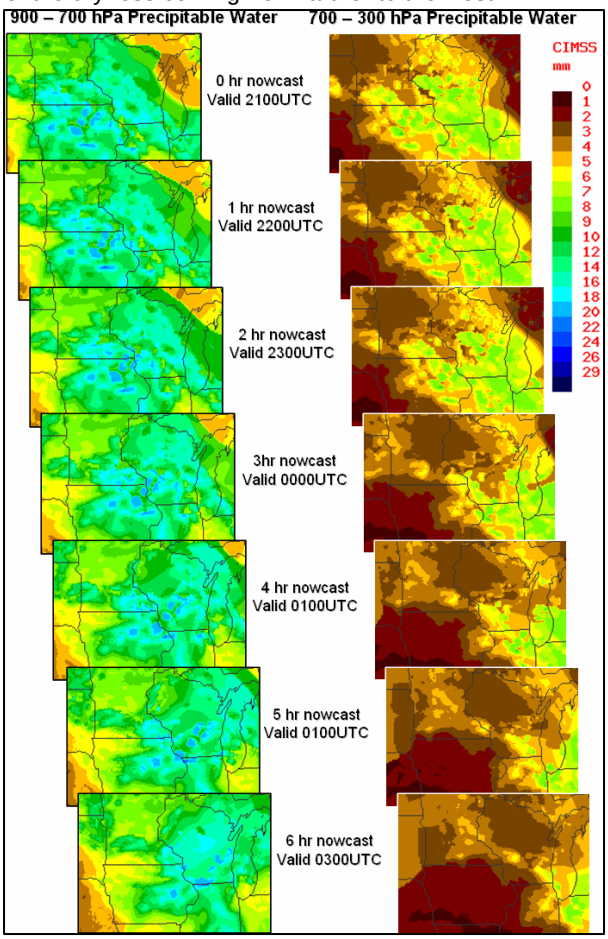

Fig. 8 Sequence of GOES DPI observations (top row) and hourly nowcasts (remainder of images in columns) for low-level moisture (left) and mid-level dryness (right column) valid from 2100 UTC 13 April to 0300 UTC 14 April 2006.

In order to depict this destabilization better, images of the difference between the low- and mid-level precipitable water were also generated. This difference can serve as a surrogate for vertical gradient of equivalent potential temperature, which is the precise measurement of convective instability.

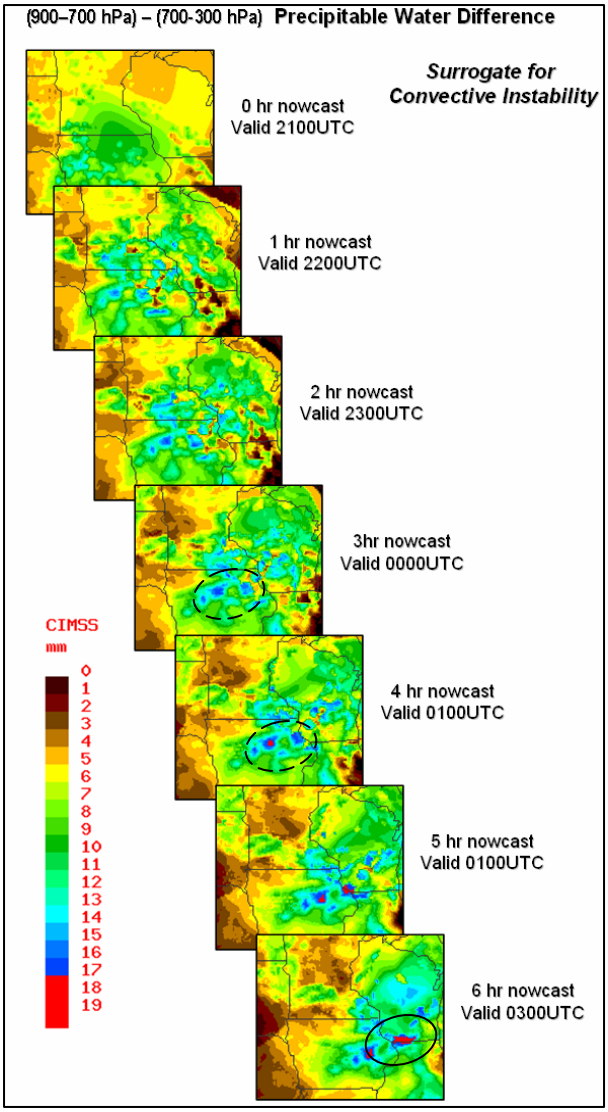

Fig. 9 Sequence of differences of GOES low-level moisture and mid-level dryness observations (top) and hourly nowcasts (remainder of images in column) valid from 2100 UTC 13 April to 0300 UTC 14 April 2006. Large differences (blue and bright red colors) indicate greater convective instability.

Note the high correlation between the 3- and 4-hr nowcasts of convective instability over central IA (development of isolated dark blue region highlighted in ovals) and the development of convection observed there at 0015 UTC in figure 6. Even more impressive is the development of the bright red band of extreme vertical moisture differences in the 6-hr nowcast over southwestern-most WI by 0300 UTC, coincident with the formation of the severe hail storms observed in that area. None of this information about the timing and location of of isolated severe convective potential would have been apparent without the nowcasts of GOES DPI products, since the DPI products are not used in operational NWP systems over land and since the DPI data at the time of convection are often masked by cirrus clouds

4. SUMMARY

A new method for objective nowcasting has been presented which uses lagrangian approaches to the numerical forecasting problem rather than the traditional Eulerian techniques. The method is advantageous in that is extremely computationally efficient, is able to retain sharp gradients and observed maxima and minima, and has the capability of providing frequent and timely updates to guidance provided by operational forecast models – using perishable observations that are not typically included in NWP systems. Both analytical and real-data tests have shown the potential of the system. The approach extends the utility of GOES DPI products (not used in NWP models over land) from observational data into objective tools that can anticipate details about the timing and location of convection 3-6 hours in advance, even after the IR observations themselves may no longer be available in the areas of severe weather due to cloud development. In order to provide consistency for operational forecasters between observations and nowcasting products, it is essential that DPI nowcasts are presented in the same form as the observed DPIs themselves.

Areas of future work include:
- Optimizing wind level selection to match satellite channel weighting and using equivalent potential temperature as the conservative transport variable,
- Additional improvements, to the 'data aging' and 'continuous successive image merger' visualizations
- Integrating Profiler, Aircraft and Cloud Tracked Wind data directly into the system to provide wind as well as moisture data updates, and
- Tests of the impact of higher vertical resolution AIRS soundings in better resolving the pre-convective environment and increase the use of POES data.

5. REFERENCES

Greenspan, D., 1972: A new explicit discrete mechanism with applications. J. Franklin Inst., 294, 231-240.

Kocin, P. J., L. W. Uccellini and R. A. Petersen, 1986: Rapid evolution of a jet streak circulation in a pre-convective environment. Meteorol. Atmos. Phys., 35, 103-138.

Petersen, R. A. and L. W. Uccellini, 1979: The computation of atmospheric isentropic trajectories using a 'discrete model" approach. Mon. Wea. Rev., 114, 719-735.

Wu, X., J. Li, W. Zhang, and F. Wang, 2005: Atmospheric profile retrieval with AIRS data and validation at the ARM CART Site. Advances in Atmospheric Sciences, 22, 647 - 654.4

6. ACKNOWLEDGMENTS

This research was supported by funding to CIMSS from the NOAA/NESDIS GOES-R Risk Reduction program.